PHILOSOPHICAL TRANSACTIONS OF THE ROYAL SOCIETY A MATHEMATICAL, PHYSICAL & ENGINEERING SCIENCES

Shelf Circulation Cells [and Discussion]

G. T. Csanady and M. Gacic

Phil. Trans. R. Soc. Lond. A 1981 **302**, 515-530
doi: 10.1098/rsta.1981.0180

Phil. Trans. R. Soc. Lond. A **302**, 515–530 (1981)
Printed in Great Britain

Shelf circulation cells

By G. T. Csanady

Woods Hole Oceanographic Institution, Woods Hole, Massachusetts 02543, *U.S.A.*

Considerable insight has recently been gained into the dynamics of continental-shelf circulation through a simplification of the governing equations, resulting in a parabolic equation for the pressure field. Solutions of this equation appear to model realistically important flow phenomena, notably the effects of winds and coastal geography in setting up half-open coastal circulation cells, and an associated trapped pressure field. Circulation cells should be established mainly on the inner shelf, according to theory, i.e. within about 30 km of the coast, and should be important agents of mass exchange.

In the present paper the theory of shelf circulation is reviewed with an emphasis on its most general predictions. Then the question is examined of how a considerable body of evidence on coastal sea-level variations in response to wind, longshore sea-level gradients, longshore and cross-shore currents can be interpreted in the theoretical framework.

1. Introduction

Many continental shelves are narrow bands of shallow sea with isobaths roughly parallel to the coastline over distances large compared with shelf width. Water motions along isobaths over such open shelves appear to be unhindered. A traditional approximation in modelling open-coast shelf circulation (understood here as residual or non-tidal flow) has correspondingly been the neglect of longshore pressure gradients, an approach that goes back to early workers in this century (Ekman 1905; Jeffreys 1923). As Freeman *et al.* (1957) put it, a 'mound' of water somehow generated adjacent to an open coast would rapidly propagate upcoast and downcoast, so that more persistent currents should be unaffected by longshore sea-level gradients.

Observation studies of continental-shelf circulation made within the last decade have shown that the traditional approximation is wrong, and that persistent longshore pressure gradients along open coasts play an important dynamical role. One well established instance is the mid- and outer shelf circulation along the east coast of North America north of Cape Hatteras. This consists principally of a broad, large-scale southwestward drift, the proximate cause of which is a longshore sea-level gradient of the order of 10^{-7}, or 1 cm in 100 km (Stommel & Leetmaa 1972; Scott & Csanady 1976; Csanady 1976, 1980; Flagg 1977; Chase 1979).

By what mechanism can persistent longshore pressure gradients be maintained along an open coast, contrary to intuition and the traditional approximation? The answer has been given in the last few years by the development of what might be called the (coastal or horizontal) boundary layer theory of shelf circulation. Under a realistic set of idealizations a parabolic equation is obtained for the pressure distribution over a sloping shelf (Birchfield 1972; Pedlosky 1974; Csanady 1978). Physically, this equation may be interpreted as a balance of vorticity tendencies. With a longshore pressure gradient there is associated across-isobath geostrophic flow. As fluid columns cross isobaths, the vortex lines of their planetary vorticity are stretched or compressed, i.e. vorticity of one sign or another is generated. This vorticity tendency can be balanced by the curl of bottom stress, given a suitable arrangement of streamlines. Thus given some constant forcing effect (e.g. a distribution of wind-stress), a particular steady flow pattern arises that

satisfies the vorticity tendency equation and other dynamical constraints. Associated with the pattern of circulation there is a pressure field affecting the continental shelf, with significant pressure gradients both cross-shore and longshore. For simple geometry, the basic pattern of transport (depth-averaged velocity) is typically a half-open circulation cell, hundreds to thousands of kilometres long. This is accompanied by a pressure field trapped within a nearshore band of a few tens of kilometres wide. Some calculated examples below illustrate this result (figures 2–9).

The focus of much recent work on the boundary layer theory of shelf circulation was an attempt to explain the mechanism of the pressure gradient driving the mid- and outer-shelf east coast circulation (Csanady 1978, 1979; Beardsley & Winant 1979). The more striking predictions of the theory, on the other hand, relate to the inner shelf, say the first 30 km from shore. It is over this inner shelf region that intricate transport and sea level distributions are predicted by theory for various forcing effects, mainly wind stress. It is clearly desirable to examine to what extent the considerable body of existing evidence on coastal sea levels and nearshore current observations supports the boundary layer theory of shelf circulation. This is the principal objective of the present paper.

Before the discussion of the observations, the boundary layer theory of shelf circulation will be reviewed, with emphasis on the simplest and most fundamental results, which are likely to remain true for continental shelves of widely differing topography. In view of the newness of the theoretical developments it seems desirable to start with such a review.

2. Models and equations of shelf circulation

Two shelf models of simple geometry are illustrated in figure 1. Isobaths are supposed straight and parallel to the coast. The coast is chosen to coincide with the y-axis, with positive x pointing out to sea. In the more general model (figure 1*a*) the depth H is an arbitrary monotonic function of x, $H = H(x)$, increasing from zero at the coast. Specific calculations are often made on models with a simple depth distribution, such as that shown in figure 1*b*, illustrating an inclined plane beach, $H = sx$, with s a constant slope. The curvature of the isobaths is dynamically unimportant and these are straightened out in the simple model.

The linearized shallow water equations, on integration with respect to depth, give rise to the following 'transport' equations:

$$\left.\begin{aligned} -fV &= -gH\partial\zeta/\partial x + F_x - B_x, \\ fU &= -gH\partial\zeta/\partial y + F_y - B_y, \\ \partial U/\partial x + \partial V/\partial y &= 0, \end{aligned}\right\} \tag{1}$$

where (U, V) are components of horizontal transport (depth-integrated velocity), f Coriolis parameter, g acceleration due to gravity, ζ sea-surface elevation about static equilibrium, and (F_x, F_y) components of kinematic wind stress, (B_x, B_y) those of bottom stress.

Equations (1) are taken to apply to circulation, or residual flow, from which tidal and other short-period motions have been filtered out. There are considerable inherent inaccuracies in specifying a filtered value of the bottom stress (B_x, B_y) appropriate for substitution in these equations. The following simple parametrization scheme is found to produce realistic results:

$$B_x = 0, \quad B_y = rv_b, \tag{2}$$

where r is a constant resistance coefficient with the dimension of velocity, and v_b is 'near-bottom' longshore velocity, which is calculated according to either of the following relations:

$$v_b = (g/f)\,\partial\zeta/\partial x \quad (H \text{ large}), \tag{3a}$$

$$v_b = V/H \quad (H \text{ small}). \tag{3b}$$

The depth H is judged to be 'large' or 'small' on the scale of turbulent Ekman layer depth. Where F_x (as well as B_x) is negligible, (3a) and (3b) are identical. The principal justification for neglecting B_x is that this stress component is small compared with the dominant terms in the first of equations (1), the Coriolis force and pressure gradient terms, which are usually in approximate balance, so that the longshore flow is quasigeostrophic. After taking the curl of equations (1), $\partial B_x/\partial y$ is still small compared with $\partial B_y/\partial x$ because longshore scales of variation are small compared with cross-shore scales.

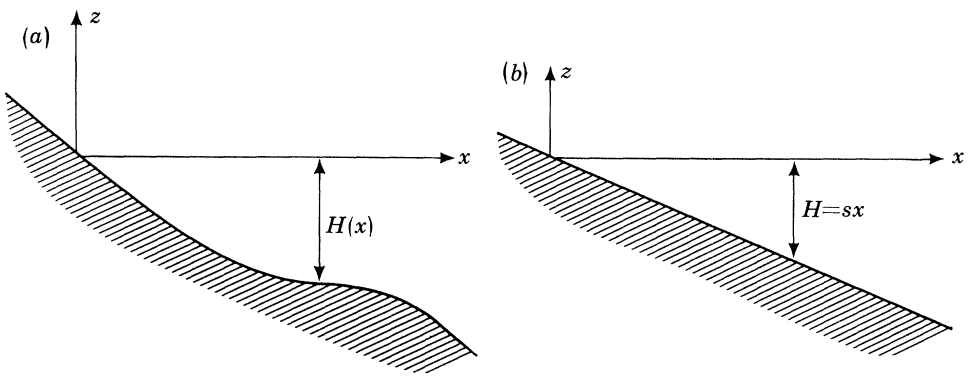

FIGURE 1. Simplified models of shelf topography. The general model (a) is more realistic than the inclined plane beach model (b), yet it gives rise to very similar circulation cells.

The important fundamental equation for the pressure field accompanying shelf circulation emerges on taking the curl of equations (1), a step that eliminates the transport components. Taking equation (3a) to represent near-bottom velocity, this equation is

$$\frac{\partial^2\zeta}{\partial x^2} + \frac{f}{r}\frac{\mathrm{d}H}{\mathrm{d}x}\frac{\partial\zeta}{\partial y} = \frac{f}{rg}W, \tag{4}$$

where

$$W = \partial F_y/\partial x - \partial F_x/\partial y \tag{4a}$$

is the wind-stress curl. Physically equation (4) may be viewed as a vorticity-tendency balance (multiplied by the factor f/rg), the terms on the left being bottom-stress curl and a vortex stretching term associated with fluid columns moving across isobaths. Other forcing terms arise in very shallow water where equation (3b) governs bottom stress, and in a nonhomogeneous fluid, within which horizontal density gradients are present. The basic character of the solutions of equation (4) remains the same in such more complex cases, being impressed by the homogeneous terms on the left. Where the forcing terms on the right vanish, the vorticity-tendency balance is between bottom-stress curl and vortex stretching, as mentioned in the Introduction.

Boundary conditions have to be specified at the coast and either at the shelf edge or at large distances from the coast. At the coast the normal transport vanishes:

$$U = 0 \quad (x = 0). \tag{5}$$

With $F_x = 0$ and $H = 0$ at $x = 0$, the second of equations (1) yields

$$F_y = B_y = (rg/f)\,\partial\zeta/\partial x \quad (x = 0), \tag{5a}$$

with the use of equation (3*a*).

In simple shelf models the other boundary condition is usually imposed at infinity, a coastally trapped field being postulated:

$$\zeta = 0 \quad (x \to \infty). \tag{6}$$

To find a solution of equation (4) it is also necessary to prescribe an 'initial' distribution:

$$\zeta = \zeta_0(x) \quad (y = 0). \tag{7}$$

A non-vanishing distribution of positive ζ_0 may be thought of as a 'mound' of water somehow maintained near $y = 0$.

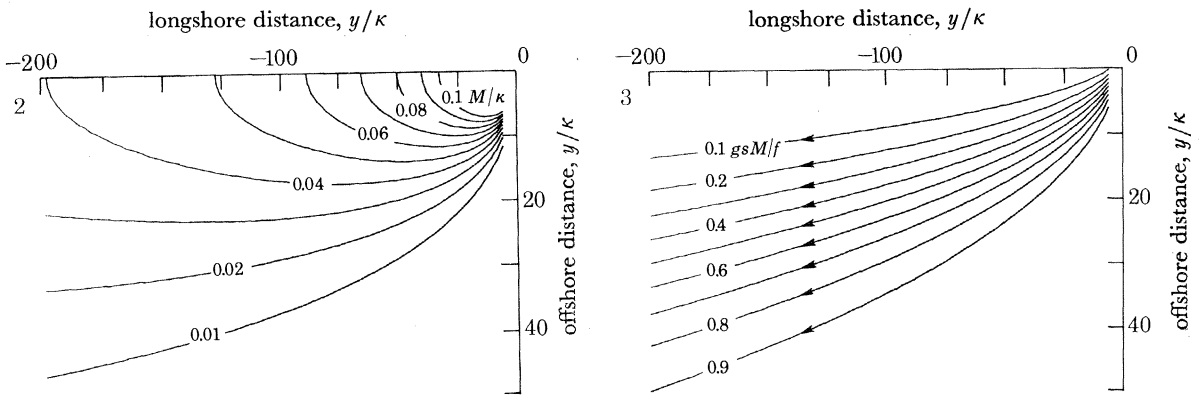

FIGURE 2. Contours of constant elevation in pressure field of coastal mound. Distances are given as multiples of $\kappa = r/fs$, or equivalent 'conductivity', a typical value of which is 1.6 km. Cross-shore distances have been stretched by a factor of $2\frac{1}{2}$. Elevations are given as multiples of M/κ, where M is the total excess fluid in the mound (equation (9)).

FIGURE 3. Transport streamlines in circulation cell of coastal mound.

Equation (4) is parabolic, of the same form as the one-dimensional heat conduction equation, with negative y playing the role of time. Many general properties of the solutions of this equation may be deduced from the heat conduction analogy. The key principle to keep in mind is that any forcing effect acting at $y = y'$ only affects 'forward' portions of the coast, $y < y'$. The equivalent 'conductivity' is $\kappa = r/fs$, which in this equation has the dimension of length.

2.1. *Initial mound of water*

The character of the solutions of equation (4) is best illustrated further by some examples calculated for the simple model of figure 1*b* and simple prototypes of forcing. Figures 2 and 3 show the pressure and streamline fields arising from the maintenance of a mound of water ($\zeta > 0$ for $0 \leqslant x \leqslant l$) at $y = 0$, with all forcing terms vanishing. The physical cause of the mound may be shoreward Ekman transport at $y > 0$ (i.e. over the 'backward' portion of the coast, see the next section), or river inflow, or something else. The streamlines are those of transport, i.e.

$$U = \partial\psi/\partial y, \quad V = -\partial\psi/\partial x. \tag{8}$$

From equation (4) it is easy to show that the volume of water in the mound is conserved:

$$M = \int_0^\infty \zeta \, dx = \text{constant}. \tag{9}$$

The general solution for an arbitrary initial distribution $\zeta_0(x)$ is easily written down, but it is sufficiently instructive to consider the case when the mound is concentrated within a small distance l from the coast at $y = 0$. At $-y \gg l$ the pressure and flow fields are given then by the simple source solution:

$$\left.\begin{aligned} \zeta &= \left(\frac{2}{\pi}\right)^{\frac{1}{2}} \frac{M}{L_x} \exp\left(-\frac{x^2}{2L_x^2}\right), \\ U &= -\frac{1}{(2\pi)^{\frac{1}{2}}} \frac{gsM}{fy} \left(\frac{x}{L_x}\right)^3 \exp\left(-\frac{x^2}{2L_x^2}\right), \\ V &= -\left(\frac{2}{\pi}\right)^{\frac{1}{2}} \frac{gsM}{fL_x} \left(\frac{x}{L_x}\right)^2 \exp\left(-\frac{x^2}{2L_x^2}\right), \end{aligned}\right\} \tag{10}$$

where

$$L_x = (-2ry/fs)^{\frac{1}{2}} \tag{11}$$

is the cross-shore length scale ('trapping width') of the field.

For the transport streamline field, with $\psi = 0$ chosen to be the coast, equations (8) and (10) give

$$\psi = (gsM/f)\, \phi(x/L_x), \tag{12}$$

where

$$\phi(\xi) = \left(\frac{2}{\pi}\right)^{\frac{1}{2}} \int_0^\xi \xi'^2 \exp\left(-\tfrac{1}{2}\xi'^2\right) d\xi'$$

so that ψ is a function of x/L_x alone.

The total longshore transport is

$$Q = \int_0^\infty V \, dx = -gsM/f, \tag{13}$$

which is independent of the y-coordinate.

The transport pattern in this simplest of all circulation cells is thus characterized by constant total longshore flow. However, the width of the flow field grows as L_x, i.e. as $y^{\frac{1}{2}}$. The longshore transport V has a maximum at $x = 2\frac{1}{2}L_x$, the cross-shore transport U at $x = 3\frac{1}{2}L_x$, both being negligible close to the coast. The longshore flow may be thought of as a relatively narrow stream centred at $x = 2\frac{1}{2}L_x$.

The narrowness of the stream arises from the typical parameters characterizing continental shelves. On a broad, flat shelf at mid-latitudes the key parameters are of order $r = 0.05\,\text{cm s}^{-1}$, $f = 10^{-4}\,\text{s}^{-1}$, $s = 3 \times 10^{-3}$. These give $L_x = 18\,\text{km}$ at $-y = 100\,\text{km}$, $L_x = 60\,\text{km}$ at $-y = 1000\,\text{km}$, i.e. very slow growth in the trapping width of the flow field with increasing longshore distance, in the 'time-like' or negative y-direction.

The contours of constant pressure are long and cigar-shaped, resembling effluent plume concentration isopleths. At the coast the cross-shore gradient vanishes with the longshore velocity, while the longshore gradient is

$$\partial\zeta/\partial y = M/(2\pi)^{\frac{1}{2}} L_x(-y) \quad (x = 0). \tag{14}$$

The longshore gradient $\partial\zeta/\partial y$ vanishes at $x = L_x$ and becomes negative (i.e. opposes the flow) at greater distances. Close to shore the main balance in the longshore direction is between the pressure gradient driving the flow and the bottom stress resisting it. Beyond $x = L_x$ the Coriolis

force of cross-shore transport becomes the largest term in the longshore momentum balance and is balanced partly by the opposing pressure gradient, and partly by bottom stress. If the water at these distances is supposed to be much deeper than Ekman depth, then the part of the cross-shore transport balancing bottom stress is carried in the bottom Ekman layer. It is interesting to reflect, however, that the broadening of the flow and pressure field in the negative y-direction necessarily implies an adverse pressure gradient on the outer edges of the field, and an associated geostrophic cross-shore flow.

The above results remain valid for negative M, i.e. for a sea-level depression at $y = 0$ instead of a mound. The signs of ζ, U and V are then all reversed. Longshore transport, in particular, is in this case toward positive y, so that at $y = 0$ a quantity of water M is flowing *out* of the domain of interest, $y < 0$. To represent this situation, the arrows in figure 3 on the streamlines should be reversed. The physical interpretation is that the fluid removed at $y = 0$ is gathered from a coastal boundary layer of increasing width (increasing toward negative y, as before). At the outer fringes of the field there is now shoreward flow, first mainly in the frictionless interior, then closer to shore mainly in the bottom Ekman layer.

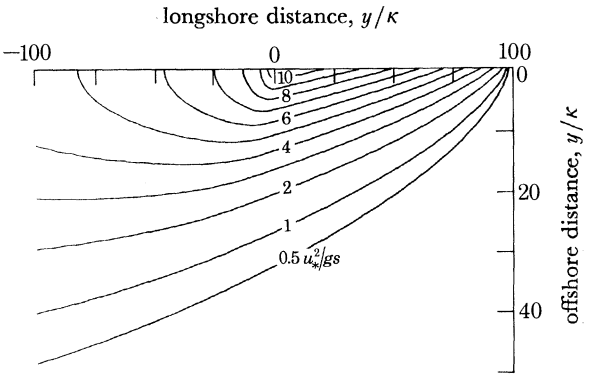

FIGURE 4. Contours of constant elevation due to longshore wind for $0 < y < 100$.

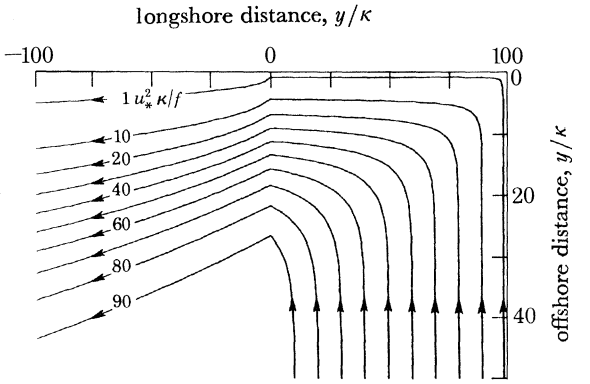

FIGURE 5. Transport streamlines corresponding to figure 4.

2.2. *Wind stress along portion of coast*

The question of what agency first generates a mound is addressed by a simple 'square-wave' model of longshore wind stress distribution:

$$\left.\begin{aligned} F_y &= -u_*^2 \quad (0 \leqslant y \leqslant Y), \\ F_y &= 0 \qquad (y \leqslant 0), \end{aligned}\right\} \tag{15}$$

or the wind blowing along a portion of the coast only. For the portion $y \leqslant 0$ the results of the previous section apply. Here the main interest is on the 'backward' portion where the wind blows.

The pressure and streamline fields for this case are shown in figures 4 and 5. The equations describing the fields have been given in Csanady (1978) (see also the discussion by Winant (1979)).

At the coast, the longshore velocity is u_*^2/r, to negative y, in accordance with the boundary condition (5a). Far from the coast transport is shoreward, with the transport streamlines evenly spaced, representing surface layer Ekman transport in the quantity u_*^2/f. In between, the average longshore velocity (V/H) distribution is self-similar, monotonically reducing from the maximum

value at the coast as its range grows with the scale L_x. The total longshore transport correspondingly grows as it absorbs the arriving Ekman transport.

For typical values of the parameters ($r = 0.05\,\mathrm{cm\,s^{-1}}$, $f = 10^{-4}\,\mathrm{s^{-1}}$, $s = 3 \times 10^{-3}$) at a distance $Y - y = 100\,\mathrm{km}$ from the beginning of the square wave, the width scale of the flow, L_x, is of the order of 30 km, and the coastal longshore gradient $\partial\zeta/\partial y|_0$ with $u_*^2 = 1\,\mathrm{cm^2\,s^{-2}}$ is of order 10^{-7}, or 1 cm in 100 km. The longshore gradient retains the same sign, opposing the applied wind stress everywhere. Physically, the existence of this gradient is a consequence of the build-up of coastal sea level, necessary to accommodate the arriving Ekman transport in a continually broadening longshore current. Note that the build-up occurs not in time, but in the time-like negative y-direction of the coast.

For wind pointing into the opposite, positive y-direction the signs change in the equations describing the field, so that a coastal sea-level depression develops gradually, *still in the negative y or time-like direction*. The physical reason is exactly the same as before, the coastal sea-level drop reflecting geostrophic balance of a longshore current of increasing width, directed now to positive y. The arrows on the streamlines in figures 4–5 reverse.

At $y = 0$, where the wind stops acting, the pressure gradient at the coast abruptly reverses sign, and for $y < 0$ the conditions discussed in the previous section prevail. Near the coast the pressure gradient drives the flow against bottom friction, but the velocity drops to zero in a nearshore band of increasing width. The scale of this, L_x^*, is the same as the scale of the field of a mound, given by equation (11). Because $L_x^* < L_x$, a second or 'internal' boundary layer may be said to form alongshore, growing in the negative y-direction. As discussed in the previous section, this internal boundary layer growth forces the longshore current further and further offshore.

A generalization of this model allows one to answer immediately the question of what happens along a coastline subject to a piecewise-constant longshore distribution of wind stress. The contribution of each piece of coastline may be calculated as above. At any given location, the flow is the sum of contributions from all 'backward' sections. Since at $y < 0$ in figures 4 and 5 an internal boundary layer appears, growing towards negative y as $(-2ry/fs)^{\frac{1}{2}}$, one infers that with many active backward sections there are many internal boundary layers. The effect of distant sections (those lying towards large positive y) is, however, decreasingly significant. These backward sections also affect increasingly the outer (high x) portions of the shelf. In each internal boundary layer the flow is forward or backward according to whether the section where it originated was subject to inward or outward Ekman transport.

2.3. *Spacewise periodic longshore wind stress*

To expand on the effects of wind stress variations along the coast, a fairly complex coastline along which the wind blows both in the forward and the backward direction may be modelled by periodic forcing:

$$F_y = u_*^2 \cos ky, \tag{16}$$

with k the longshore wavenumber of the wind field. The appropriate pressure and streamline fields are illustrated in figures 6 and 7, and are described by equations given in Csanady (1978).

The pressure distribution illustrates particularly clearly how sections further and further backward progressively influence outer domains of the shelf, with rapidly reducing intensity, as remarked at the end of the last section. The associated transport streamline pattern is simpler mainly because of the regularity of a periodic arrangement and shows that the total Ekman transport arriving at some portion of the coast becomes longshore current toward negative y,

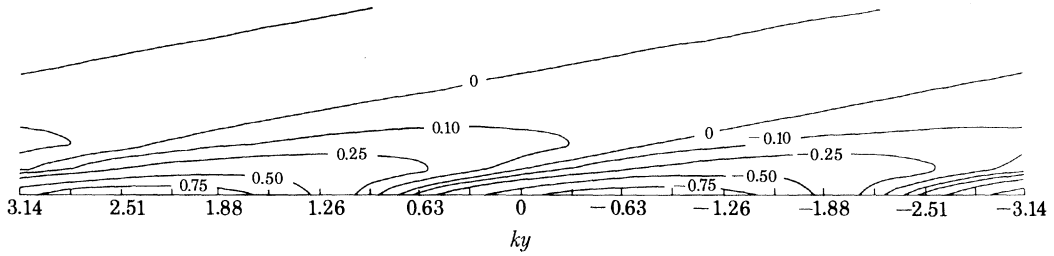

FIGURE 6. Contours of constant elevation due to periodic longshore wind stress (from Csanady 1978).

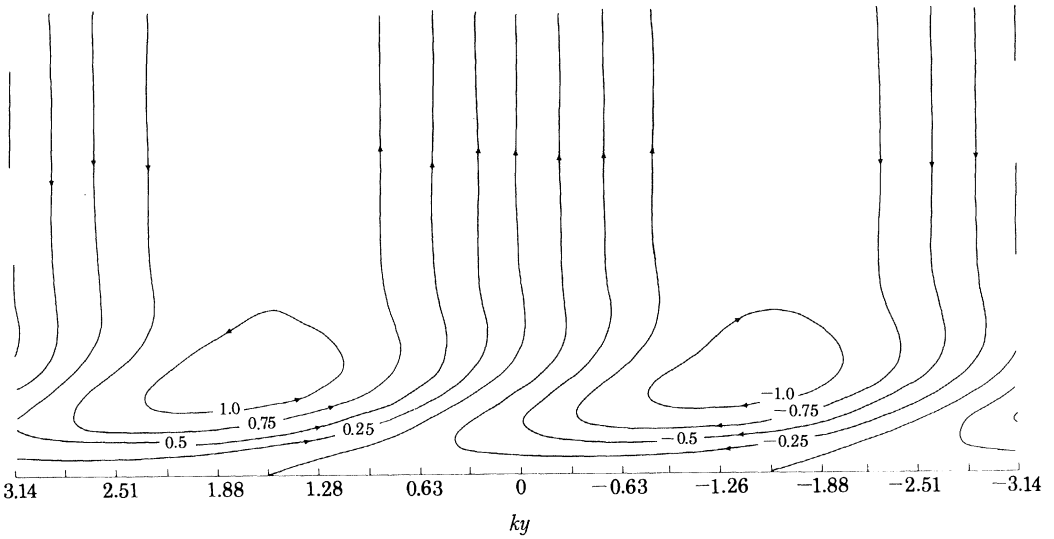

FIGURE 7. Transport streamlines corresponding to figure 6 (periodic longshore wind stress (Csanady 1978)).

and then leaves the coast again where Ekman transport is directed offshore. Longshore gradients are dynamically significant and cross-shore transport is relatively large in some places even at short distances from the coast. The amplitudes of coastal sea-level elevation, longshore velocity and longshore pressure gradient are given by

$$\left.\begin{aligned} \zeta_a &= \frac{u_*^2}{g}\frac{fL}{r}, \\ v_a &= u_*^2/r, \\ \left.\frac{\partial\zeta}{\partial y}\right|_a &= \frac{ku_*^2}{g}\frac{fL}{r}, \end{aligned}\right\} \tag{17}$$

where $L = (2r/fks)^{\frac{1}{2}}$ is the scale of nearshore trapping. For typical values of the parameters ($u_*^2 = 1\,\mathrm{cm^2\,s^{-2}}, f = 10^{-4}\,\mathrm{s^{-1}}, r = 0.05\,\mathrm{cm\,s^{-1}}, s = 3\times10^{-3}, k = 2\pi/2000\,\mathrm{km}$) the above formulae give a trapping width scale, L, for the field of 33 km and typical amplitudes of $\zeta_a = 6.5\,\mathrm{cm}$, $v_a = 20\,\mathrm{cm\,s^{-1}}$, $\partial\zeta/\partial y|_a = 2\times10^{-7}$, or 2 cm in 100 km.

2.4. *Periodic cross-shore wind*

Similar calculations may be made for periodic cross-shore winds. A computational difficulty arises at the coast $H = 0$, where the linearized equations become physically unrealistic. The resolution of such difficulties was discussed in Csanady (1980). Here the resulting pressure field and streamline distributions are illustrated in figures 8 and 9.

Near the coast, the pressure field shows features of wind set-up, sea level rising where the wind blows onshore, dropping where it is offshore. Far from the shore cross-shore winds produce longshore Ekman transport. Given a cross-shore wind-stress field varying in the longshore direction as $\cos ky$, the Ekman transport is convergent–divergent and forces a cross-shore flow pattern, associated with a pressure field that does not vanish at infinity.

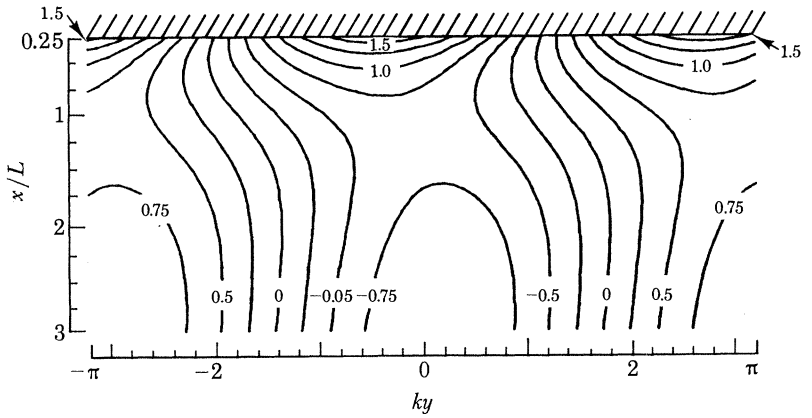

FIGURE 8. Contours of constant elevation due to periodic cross-shore wind (from Csanady 1980).

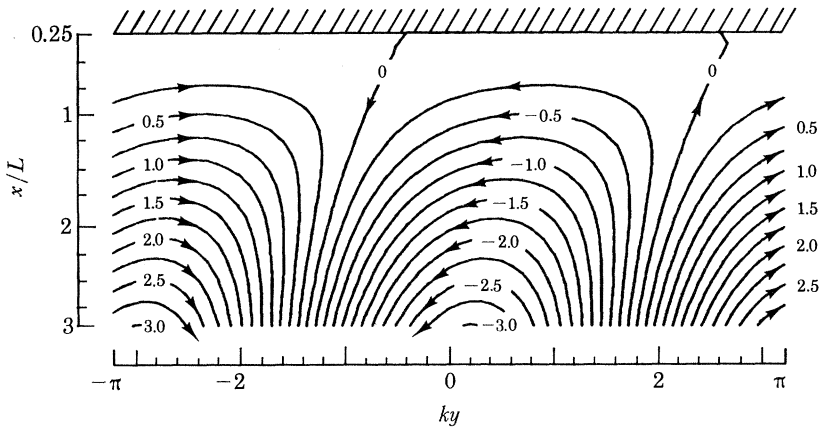

FIGURE 9. Transport streamlines corresponding to figure 8 (periodic cross-shore wind (Csanady 1980)).

At large distances from the coast this model becomes unrealistic, but the near-shore amplitudes of sea-level elevation, etc., presumably remain useful and are given by

$$\left.\begin{aligned} \zeta_a &= u_*^2/gs, \\ V_a &= u_*^2/f, \\ \partial\zeta/\partial y|_a &= ku_*^2/gs. \end{aligned}\right\} \tag{18}$$

The sea level and pressure gradient amplitudes are similar to those for longshore wind (equation (19)) except for a factor of $\frac{1}{2}kL$. A typical value of the quantity $\frac{1}{2}kL$ is 0.05, so that cross-shore winds are much less effective in building coastal sea level than longshore winds. It is noted here, however, that the 'typical' k used in these estimates was small, appropriate to a large weather system affecting a long straight coast. With a much larger k, the relative importance of cross-shore winds should increase.

The preceding sections should place in perspective the theory of shelf circulation cells. The remaining sections will address the question of to what extent the theory can be quantitatively related to observation.

3. Coastal sea level

The above theoretical models are all highly idealized and cannot be expected to apply directly and in all details to any given real situation in the coastal ocean. However, it may be possible to discern in the observational evidence certain key signatures of shelf circulation cells and of the associated coastally trapped pressure fields. These include, for example, preferential response to longshore rather than cross-shore wind stress in large weather systems, the appearance of longshore pressure gradients of a magnitude about that expected from theory, significant cross-shore

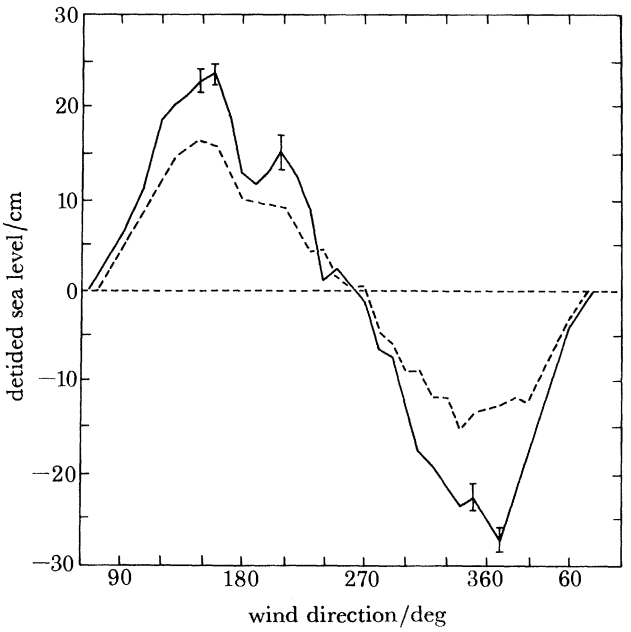

Figure 10. Detided sea level at a tide gauge on the West Florida shelf (Cedar Key) against wind direction (from Cragg & Sturges 1974). ——, Wind speed 4.5 m s^{-1}; – – –, 3.5 m s^{-1}.

transport relatively close to shore, and the influence of a disturbance spreading in the 'forward' or negative y-direction (in the Northern Hemisphere). One may expect to observe such effects where bottom friction plays a dominant role in determining the response of the coastal ocean to forcing, i.e. over broad and flat continental shelves ('Atlantic'-type shelves) subject to strong tidal currents.

Statistical analyses have recently been published of nontidal coastal sea-level changes associated with winds over Atlantic-type shelves (Cragg & Sturges (1974), the West Florida shelf; Wang (1979), Chase (1979), Noble & Butman (1979) and Sandstrom (1980), the North American east coast shelf north of Cape Hatteras). The main signal in such wind-induced sea-level variations is due to extratropical cyclones passing over the area. The typical diameter of weather systems of this kind is of the order of 1000 km.

As an extratropical cyclone passes over a long, almost straight segment of the coast, each location is exposed to roughly the same history of forcing. In some configuration of coast and weather system the maximum response should be approached at each location. Hence the

statistically determined response amplitude should be comparable with the amplitudes ζ_a, v_a, etc. of the theoretical models almost without regard to phase. However, at locations close to sharp changes in coastline orientation the geography of the coast should become important. For example, near the tip of the Florida peninsula a wind blowing from the northwest is directed toward negative y (in a coordinate system defined analogously to that of the simple models) on the east coast, and toward positive y on the west coast, with a rapid variation in between. Similar, and even more complex, considerations apply in the northeast sector of the east coast of the U.S.A., in the region of the Gulf of Maine or around Long Island. In such more complex situations one must think of at least two important longshore scales, one being the weather-cycle scale, the other the distance to the closest sharp corner of the coast.

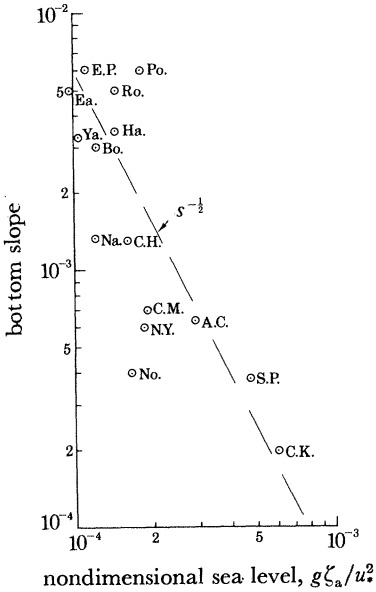

FIGURE 11. Sea-level response to unit wind stress against bottom slope of coastal region, for various tide gauges on West Florida and east coast shelves. Key: A.C., Atlantic City; Bo., Boston; C.H., Cape Hatteras; C.K., Cedar Key; C.M., Cape May; Ea., Eastport; E.P., Eddy Point; Ha., Halifax; Na., Nantucket; No., Norfolk; N.Y., New York; Po., Portland; Ro., Rockland; S.P., St Petersburg; Ya., Yarmouth.

Observing the necessary caveats, it is nevertheless possible to distill from the statistical analyses important generalizations and to seek an interpretation of them in terms of the theory discussed earlier.

3.1. *Sea level and longshore wind*

The proposition that detided sea level responds mainly to longshore wind is by now well established, from much early work, as well as from the more recent studies quoted. An impressive illustration is figure 10 taken from Cragg & Sturges (1974), who have plotted sea-level response against wind direction (for constant wind speed) for a location on the West Florida shelf. The peak occurs when the wind is parallel to the coast.

The amplitude of the sea-level rise should, according to the theory, be proportional to wind stress, given otherwise the same parameters, mainly resistance coefficient r, wavenumber of forcing k, and bottom slope s. Noble & Butman (1979) demonstrate this in detail.

On forming the nondimensional coefficient

$$a = g\zeta_a/u_*^2, \tag{19}$$

the influence of wind stress is removed from coastal sea-level amplitude, which should then depend on r, k and s. Suppose that over the east coast and Florida shelves there are no systematic variations in either bottom friction coefficient r or weather system wavenumber k, then the coefficient a should vary mainly with bottom slope s, and according to simple theory as $s^{\frac{1}{2}}$. This would apply to locations suitably distant from sharp corners of the coastline. Noble & Butman (1979) give a table of the coefficient a, multiplied by a dimensional factor. The same coefficient is also readily computed from the data of Cragg & Sturges (1974). These are plotted in figure 11 against bottom slope s, the latter defined as 40 m depth divided by the distance of the 40 m isobath from the coast. This particular depth was chosen as a typical mid-shelf value, but other choices up to 100 m give similar results, although different quantitative values for s. Some scatter is expected in such a graph for various reasons, and yet a rough agreement with the theoretical trend is evident.

3.2. *Longshore pressure gradients*

Longshore gradients of sea level were seen above to be key features of coastally trapped pressure fields. Coastal sea-level observations made at several tide gauges should in principle reveal such gradients. However, in practice the magnitude of the level-difference signal is small, typically a few centimetres, and its identification requires a particularly effective filtering-out of sea-level variations due to other causes. Along the east coast, of the U.S.A., Wang (1979) finds such sea-level gradients to be significantly related to longshore wind stress only over the southern Long Island coast. Along the same piece of coastline, Chase (1979)and Pettigrew (1980) studied the longshore pressure gradient in greater detail. Figure 12, from Pettigrew (1980), shows the two time series in question for a brief period. Even a visual inspection leaves little doubt about the relation between the two. Regression analysis by Pettigrew yields the result that a $0.1\,\mathrm{N\,m^{-2}}$ ($1\,\mathrm{dyn\,cm^{-2}}$) wind stress evokes a 3×10^{-7} longshore level gradient, opposing the wind stress. Cragg & Sturges (1974) find on the West Florida shelf a gradient of about 7.5×10^{-7} for $0.1\,\mathrm{N\,m^{-2}}$ longshore wind.

The quantitative relations between wind stress and coastal sea level, and between wind stress and longshore level gradient, can be used to calculate the longshore wavenumber k, if the first and third of equation (17) are supposed apply. More directly, if one writes for the amplitude of longshore level gradient

$$\partial\zeta_a/\partial y = k\zeta_a, \tag{20}$$

one has at once

$$\frac{g}{u_*^2}\frac{\partial\zeta_a}{\partial y} = k\frac{g\zeta_a}{u_*^2} = ak, \tag{20a}$$

where a is as defined in equations (19). With the data of Pettigrew (1980) one finds $k = 2\times10^{-8}$ $\mathrm{cm^{-1}}$, with the data of Cragg & Sturges (1974) $k = 1.5\times10^{-8}\,\mathrm{cm^{-1}}$, corresponding respectively to half wavelengths of 1500 and 2000 km. In order of magnitude, these dimensions agree with typical cyclone diameters, although they are larger.

4. Evidence of moored instruments

Sea-level observations have been taken for many years and the above analysis of subtidal-level variations could have been carried out decades ago. More recent is the evidence of moored instrumentation, deployed over inner and outer regions of Atlantic-type shelves. Bottom pressure sensors placed at varying distances from shore can answer questions regarding the extent of the

PHILOSOPHICAL TRANSACTIONS OF THE ROYAL SOCIETY A MATHEMATICAL, PHYSICAL & ENGINEERING SCIENCES

pressure field (whether trapped or not, for example) and the magnitude of cross-shore as well as longshore gradients. Moored current meter records give information on longshore velocity and transport, and less accurately, on the weaker cross-shore motions.

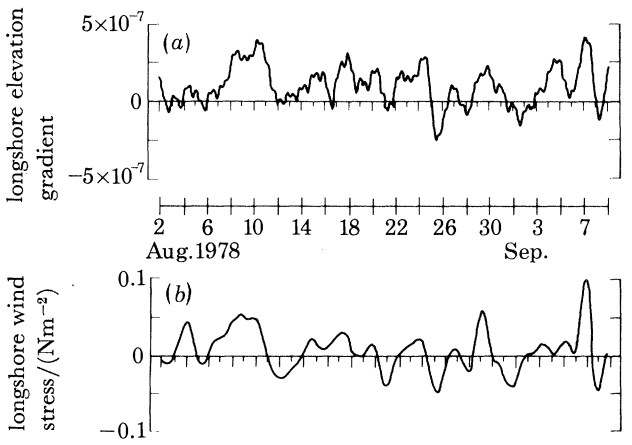

FIGURE 12. (*a*) Detided longshore pressure gradient (surface slope) and (*b*) similarly filtered wind stress along south coast of Long Island (from Pettigrew 1980).

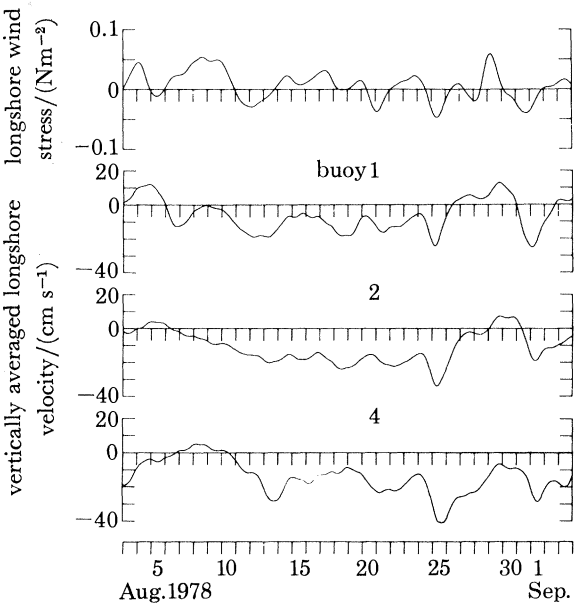

FIGURE 13. Longshore components of wind stress and depth-averaged velocity along south coast of Long Island (from Pettigrew 1980).

In a study of bottom pressure fluctuations in the Mid-Atlantic Bight in March 1974, Beardsley *et al.* (1977) have provided convincing evidence on the presence and coastal trapping of cross-shore pressure gradients. In the frequency band covering wind-induced fluctuations (2- to 13-day period) they found a r.m.s. cross-shore level gradient of about 2.2×10^{-6} between 0 and 30 km from the coast, and half that between 30 and 60 km. This corresponds to a trapping scale L of 43 km. The corresponding r.m.s. longshore velocity by geostrophic balance is about 25 cm s^{-1}

close to shore. The r.m.s. longshore gradient was about 4×10^{-7}, higher than the value found by Pettigrew for August 1978.

The most readily observable result of longshore wind stress is longshore flow. This has been reported on several occasions, on the inner shelf, for example, by Scott & Csanady (1976) or Bennett & Magnell (1979), on the outer shelf by Beardsley & Butman (1974), Beardsley *et al.* (1976) and Boicourt & Hacker (1976). Figure 13, from Pettigrew (1980), shows the association o longshore wind stress and depth-average velocity at 3, 6 and 12 km from shore off Long Island. There is an underlying trend in the velocity record unrelated to the wind. However. there is also a clear response to wind, of an amplitude of about 20 cm s^{-1} for a 0.1 N m^{-2} wind stress. By the second of equation (26) this corresponds to $r = 0.05$ cm s^{-1}, a value also roughly in accord with results of other studies.

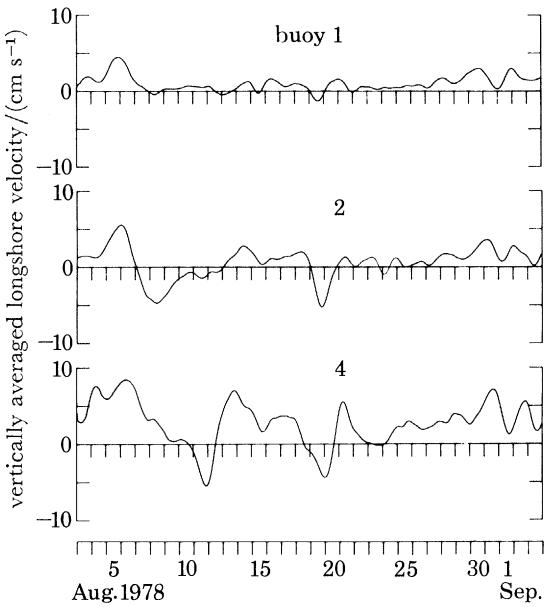

FIGURE 14. Depth-averaged cross-shore velocity along south coast of Long Island (from Pettigrew 1980).

By taking this value of r, it is possible to attempt a reconciliation of the parameters entering the theoretical model. The empirically determined value of a (equation (19) and figure 11) in the Mid-Atlantic Bight is between 1×10^{-4} and 2×10^{-4}. The first of equations (17) gives, with this a and $r = 0.05$, a trapping width of 50–100 km, i.e. higher than computed from the data of Beardsley *et al.* (1977), but of the same order. Given the crudeness of these estimates and the over-idealizations of the simple model better agreement could not be expected.

Substituting into the definition of L, one finds that $r = 0.05$ and $a = 2 \times 10^4$ ($L = 100$ km) are consistent with the previously estimated longshore wavenumber of $k = 2 \times 10^{-8}$ cm and a slope of $s = 10^{-3}$, the latter being a reasonable model of this portion of the shelf.

Non-vanishing cross-shore transport at short distances from the coast is another key signature of shelf circulation cells, and the one most directly related to their mass-exchange role. Although the conventional wisdom that U vanishes within some distance of the coast is strongly ingrained, Smith (1978, 1979, 1980) has repeatedly drawn attention to the fact that this hypothesis may have to be abandoned even at about 10 km from the coast. Smith's current meter observations along

the Texas Gulf coast showed that unreasonable assumptions would have to be made on the velocity distribution to force agreement with the zero cross-shore transport thesis. The same proposition was demonstrated in greater detail by Pettigrew (1980) for the Long Island coast. Figure 14 shows depth-average cross-shore velocity at 3, 6 and 12 km. While the values at 3 km are perhaps mostly noise, the cross-shore transports at 12 km cannot reasonably be explained away.

5. Conclusion

Space does not permit me to enter into a more detailed discussion of the longshore momentum balance that one can reconstruct from the observations or effects of cross-shore winds, or other more subtle aspects of the evidence. The brief survey above should have demonstrated that the observations conform to several key general characteristics of the models. Quantitative relations between the observed variables seem to be predictable on the basis of the theory, with the crude estimate $r = 0.05\,\mathrm{cm\,s^{-1}}$ for the bottom resistance coefficient. It is reasonable to conclude that the boundary layer theory of shelf circulation constitutes an appropriate theoretical framework for the interpretation of detided coastal sea level and coastal current observations.

This work was supported by the U.S. Department of Energy, under a contract entitled Coastal-Shelf Transport and Diffusion. Mr J. H. Churchill made the computations of the elevation and streamline patterns.

References (Csanady)

Beardsley, R. C., Boicourt, W. C. & Hansen, D. V. 1976 In *Middle Atlantic Continental Shelf and the New York Bight* (ed. M. G. Gross), *Am. Soc. Limnol. Oceanogr., spec. Symp.* **2**, 20–34.
Beardsley, R. C. & Butman, B. 1974 *Geophys. Res. Lett.* **1**, 181–184.
Beardsley, R. C., Mofjeld, H., Wimbush, M., Flagg, C. & Vermersch, J. 1977 *J. geophys. Res.* **82**, 3175–3182.
Beardsley, R. C. & Winant, C. D. 1979 *J. phys. Oceanogr.* **9**, 612–619.
Bennett, J. R. & Magnell, B. A. 1979 *J. geophys. Res.* **84**, 1165–1175.
Birchfield, G. E. 1972 *J. phys. Oceanogr.* **2**, 355–362.
Boicourt, W. C. & Hacker, P. W. 1976 *Mém. soc. R. Sci. Liège*, ser. 16, **10**, 187–200.
Chase, R. R. P. 1979 *J. geophys. Res.* **84**, 4898–4904.
Cragg, J. & Sturges, W. 1974 Technical Report, Florida State University, Tallahassee, Florida, no. 32306 (51 pp.).
Csanady, G. T. 1976 *J. geophys. Res.* **81**, 5389–5399.
Csanady, G. T. 1978 *J. phys. Oceanogr.* **8**, 47–62.
Csanady, G. T. 1979 *J. geophys. Res.* **84**, 4905–4915.
Csanady, G. T. 1980 *J. geophys. Res.* **85**, 1076–1084.
Ekman, V. W. 1905 *Ark. Mat. Astr. Fys.* **2**, no. 11 (52 pp.).
Flagg, C. N. 1977 Ph.D. thesis, Massachusetts Institute of Technology/Woods Hole Oceanographic Institution, W.H.O.I. ref. 77–67 (207 pp.).
Freeman, J. C., Baer, L. & Jung, G. H. 1957 *J. mar. Res.* **16**, 12–22.
Jeffreys, H. 1923 *Phil. Mag.* **45**, 114–125.
Noble, M. & Butman, B. 1979 *J. geophys. Res.* **84**, 3227–3236.
Pedlosky, J. 1974 *J. phys. Oceanogr.* **4**, 214–226.
Pettigrew, N. R. 1980 Ph.D. thesis, Massachusetts Institute of Technology/Woods Hole Oceanographic Institution (262 pp.).
Sandstrom, H. 1980 *J. geophys. Res.* **85**, 461–468.
Scott, J. T. & Csanady, G. T. 1976 *J. geophys. Res.* **81**, 5401–5409.
Smith, N. P. 1978 *J. geophys. Res.* **83**, 6047–6051.
Smith, N. P. 1979 *J. phys. Oceanogr.* **9**, 624–630.
Smith, N. P. 1980 *J. geophys. Res.* **85**, 1531–1536.
Stommel, H. & Leetmaa, A. 1972 *Proc. natn. Acad. Sci. U.S.A.* **69**, 3380–3384.
Wang, D.-P. 1979 *J. mar. Res.* **37**, 683–697.
Winant, C. D. 1979 *J. phys. Oceanogr.* **9**, 1042–1043.

PHILOSOPHICAL TRANSACTIONS OF THE ROYAL SOCIETY A MATHEMATICAL, PHYSICAL & ENGINEERING SCIENCES

Discussion

M. Gačić (*Institute of Oceanography and Fisheries*, P.P. 114, 58000 *Split*, *Yugoslavia*). Our calculations of multiple correlations between sea level, atmospheric pressure, and longshore and cross-shore wind-stress components for the Adriatic sea show that the cross-shore wind-stress component has slightly more influence on sea-level oscillations during the summer than the longshore component. During the winter the influence of the longshore wind-stress component is ten times that of the cross-shelf component. All these calculations were done for time-scales larger than a day, daily and tidal oscillations being eliminated from time series. Could Dr Csanady explain in terms of the presented model, the prevalence of the influence of the cross-shore wind stress during summer?

G. T. Csanady. It is not possible to comment on your results without studying the problem in detail. The Adriatic Sea, however, is a narrow enclosed basin in which 'cross-shore' wind in one location is directed longshore in another. The application of similar notions to the Great Lakes has, generally, been fruitful, but there have been some complications especially during summer conditions (see G. T. Csanady & J. T. Scott, *J. geophys. Res.* **85**, 2797–2812 (1980)).

PHILOSOPHICAL TRANSACTIONS OF THE ROYAL SOCIETY A MATHEMATICAL, PHYSICAL & ENGINEERING SCIENCES